Temperature and composition of the Earth's core

Article *in* Contemporary Physics · March 2007

DOI: 10.1080/00107510701529653

CITATIONS
119

READS
7,212

2 authors, including:

Geoffrey David Price
University College London
302 PUBLICATIONS **13,644** CITATIONS

SEE PROFILE

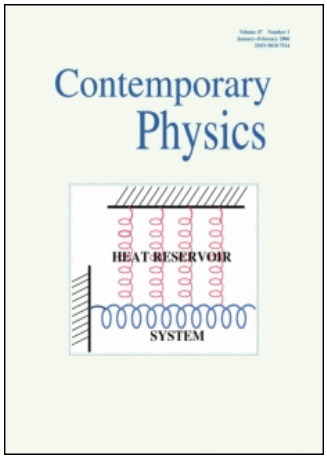

Contemporary Physics
Publication details, including instructions for authors and subscription information:
http://www.informaworld.com/smpp/title~content=t713394025

Temperature and composition of the Earth's core

D. Alfè [abc]; M. J. Gillan [ac]; G. D. Price [b]
[a] Department of Physics and Astronomy, University College London, London, UK
[b] Department of Earth Sciences, University College London, London, UK
[c] London Centre for Nanotechnology, University College London, London, UK

Online Publication Date: 01 March 2007
To cite this Article: Alfè, D., Gillan, M. J. and Price, G. D. (2007) 'Temperature and composition of the Earth's core', Contemporary Physics, 48:2, 63 - 80
To link to this article: DOI: 10.1080/00107510701529653
URL: http://dx.doi.org/10.1080/00107510701529653

Contemporary Physics, Vol. 48, No. 2, March – April 2007, 63 – 80

Taylor & Francis
Taylor & Francis Group

Temperature and composition of the Earth's core

D. ALFÈ*†‡§, M. J. GILLAN†§, and G. D. PRICE‡

†Department of Physics and Astronomy, University College London, Gower Street, London WC1E 6BT, UK
‡Department of Earth Sciences, University College London, Gower Street, London WC1E 6BT, UK
§London Centre for Nanotechnology, University College London, Gower Street, London WC1E 6BT, UK

(*Received 27 April 2007; in final form 21 June 2007*)

The Earth's core is a ball of swirling hot metal at the centre of our planet, with a radius roughly one half of the Earth's radius. It is formed by two parts: a solid inner core, with a radius of 1221 km, surrounded by a shell of liquid which extends up to 3480 km from the centre. It is widely believe that the Earth's core is mainly formed by iron, or iron with up to 5 – 10% of nickel. It is also known that the core must contain a significant fraction of light impurities, in the region of 2 – 3% in the solid and 6 – 7% in the liquid. The nature of these light impurities is unknown. The temperature of the core is also inaccessible to direct probing. Here we present a theoretical study on the temperature and the composition of the Earth's core. The investigation is based on the application of the implementation of quantum mechanics known as density functional theory. We shall show that these techniques are very accurate at predicting the properties of iron, and therefore can be usefully used to study the properties of the core. We show that by combining these techniques with direct observations it is possible to predict the temperature of the core, in particular the temperature at the boundary between the solid and the liquid core (the ICB), and put constraints on its composition. The result of this study is that the temperature of the ICB is probably in the region of 5400 – 5700 K and that the outer core contains a significant fraction (8 – 13%) of oxygen. As the Earth cools down the solid core grows and expels oxygen in the liquid. Since oxygen is lighter than iron it rises in the liquid, and its gravitational energy is available to drive the convective motions in the liquid core that are responsible for the generation of the Earth's magnetic field.

1. Introduction

Ever since the publication of *Voyage au centre de la Terre* (Journey to the Centre of the Earth) by Jules Verne in 1864 human knowledge about the interior of our planet has certainly improved significantly. However surprising this might seem though, virtually all our current knowledge is based on indirect evidence, as the deepest holes that mankind has been able to drill are only a few kilometres deep (the record belongs to the Kola Superdeep Borehole on the Kola Peninsula, a project started in 1970 which achieved a depth of 12 262 m in 1989 [1]).

Given the great success of humankind at exploring space in the past few decades, one might be forgiven for asking why similar achievements have not been obtained in directly exploring the interior of our own planet. There

*Corresponding author. Email: d.alfe@ucl.ac.uk

Contemporary Physics
ISSN 0010-7514 print/ISSN 1366-5812 online © 2007 Taylor & Francis
http://www.tandf.co.uk/journals
DOI: 10.1080/00107510701529653

are two main reasons for this: high pressure and high temperature. The conditions of temperature and pressure under which we have evolved ($P = 1$ bar, $T = 300$ K) are, in a sense, very close to those found in outer space, where the pressure is (nearly) zero and the temperature can only change by a few hundred degrees (the absolute minimum of temperature is 0 K), provided we do not go too near to stars. For this reason humankind is being very successful at exploring space, including the outer planets in the solar system, and has even been able to send some probes into interstellar space with the *Voyager 1/2* missions which are still pacing their way towards other stars and planetary systems. When it comes to going inside the Earth though the rapid increase in temperature and pressure with depth make the challenges quickly unsurmountable, although there have been suggestions on how one might envisage sending a probe even to the Earth's core [2].

We therefore owe essentially all our knowledge about the interior of the Earth to indirect measurements based on the observation of seismic events. When an earthquake strikes somewhere near the surface of the Earth (earthquakes are due to fractures in the crust and the upper mantle, and most of them are relatively shallow, though they can happen even up to 800 km depth) seismic waves travel through the Earth, and their speed and directions depend on the characteristics of the materials they travel into. Monitoring stations are distributed all around the globe, and by analysing the travel times, the frequencies and the amplitudes of the seismic waves that arrive at these stations, it is possible to infer the properties of the materials inside the Earth (see figure 1). Coupling these with measurements of *free oscillations* (i.e. global oscillations of the Earth, which after an earthquake rings like a bell) and the Earth's angular momentum, we now know that the structure of the Earth can be broadly described in terms of three main shells. The outermost is the crust, with a thickness of only a few tens of kilometres, and it is mainly formed by silicates (rocks). Below the crust we find the mantle, which is customarily divided into an upper mantle and a lower mantle, separated by a transition zone.

The mantle makes up most of the volume of the Earth, extending to a depth of 2870 km, almost half way towards the centre, and like the crust is also mainly formed by silicates, and in particular by $Mg(Fe)SiO_3$ with some significant fraction of $Mg(Fe)O$ and SiO_2. Below the mantle we find the core, which is divided into an outer

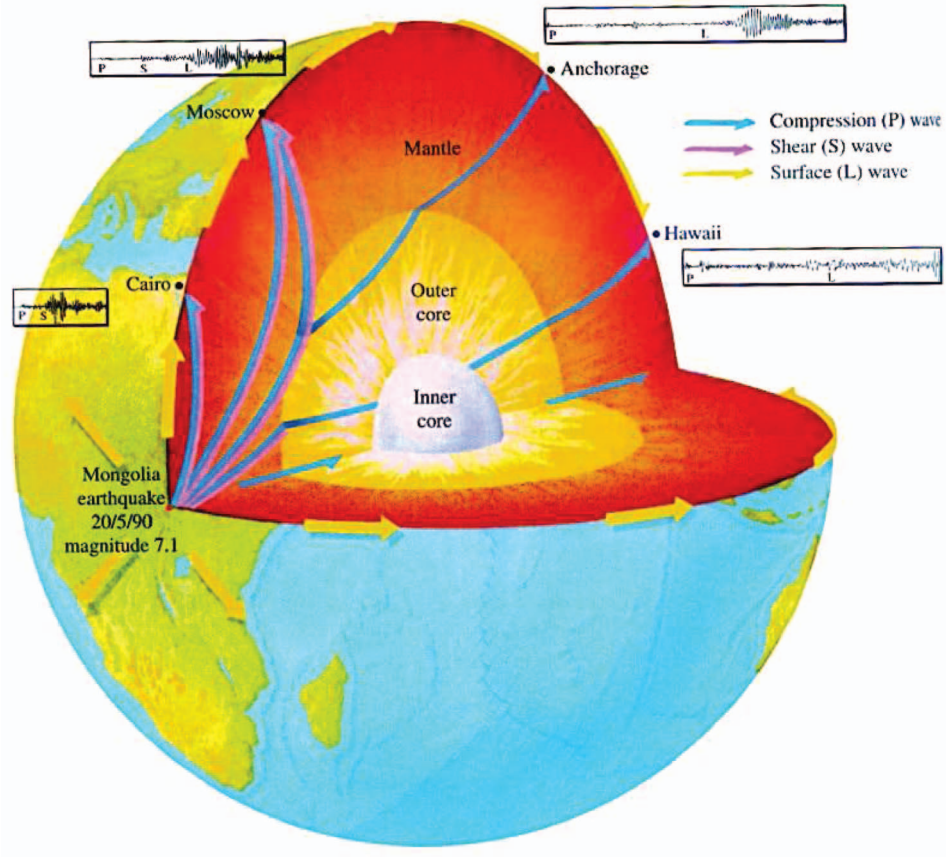

Figure 1. Earth's structure and schematic picture of travelling seismic waves inside the Earth.

liquid core extending from 2870 to 5125 km depths and an inner solid core below that, down to the centre of the Earth at 6346 km depth.

Figure 2 reports some of the *Preliminary Reference Earth Model* data, best known as PREM [3], and in particular the seismic velocities, the density and the pressure as a function of depth. The figure shows very remarked discontinuities in the seismic velocities and the density at about half of the Earth radius, where the core begins. Here Vs represent the shear waves, and Vp the pressure waves. Pressure waves are oscillations parallel to the directions of propagation, very much like sound waves. Shear waves instead have their direction of oscillation in a plane orthogonal to the direction of propagation, and for this reason cannot be supported by fluids. The disappearance of shear waves at 2870 km indicates that the core is liquid. The second interesting discontinuity is at a depth of 5125 km, where the shear waves can be supported by a solid core. The large discontinuity in the density, which essentially doubles at 2870 km, is due to the completely different nature of the core which obviously cannot be made of the same materials that make up the mantle. It is also necessary for this material to be a metal, as the only credible mechanism for the generation of the Earth's magnetic field is the presence of convective currents in the liquid part of the Earth's core.

The only metal that is abundant enough in the solar system and that almost matches the density of the core is iron, and it is widely believed today that the Earth's core is mainly made by iron, with possibly up to 10% of nickel. This is also the main composition of meteorites falling on Earth, which keep a record of the building blocks of the early solar system. Pure iron however, or the iron/nickel mixture, is too dense, and therefore the core must also contain a fraction of unknown light impurities which reduce the density by $\sim 7\%$ in the liquid with respect to the density of pure iron under the same pressure–temperature conditions. The leading light impurity candidates are S, Si and O, although also C and H have sometimes been suggested [4].

At 5125 km we find the boundary between the solid and the liquid, and a second clear discontinuity is evident; the solid core is $6.5 \pm 1.4\%$ more dense than the liquid, according to the latest estimates [5]. This discontinuity cannot be entirely attributed to the density change on melting and must be due to partition of light impurities between solid and liquid. We shall see that this partitioning plays a fundamental role in constraining the chemical composition of the Earth's core.

Understanding the Earth's core is obviously important for a number of reasons. A large part of the energy which drives the dynamics of our planet comes from the cooling of the core (a large part also comes from the decay of radioactive material in the mantle and, possibly, in the core). Moreover, the generation of the Earth's magnetic field is believed to be mainly driven by compositional convection in the liquid core, with light elements being released at the boundary between the liquid and the solid (the *inner core boundary*, or ICB) as the solid core freezes, and their gravitational energy being efficiently used to drive convection. The distribution of the temperature inside the planet, the *geotherm*, is also crucial to understand convection and heat transfer.

In order to estimate the geotherm in the core people usually assume that the liquid is in a state of turbulent convection, which implies that the distribution of the temperature in the core follows an adiabat, and this leads to the following expression for the dependence of temperature T on radius r:

$$\mathrm{d}T/\mathrm{d}r = -(\partial T/\partial p)_S \, \mathrm{d}p/\mathrm{d}r = -\rho g (\partial T/\partial p)_S = \rho g T \gamma / K_S, \tag{1}$$

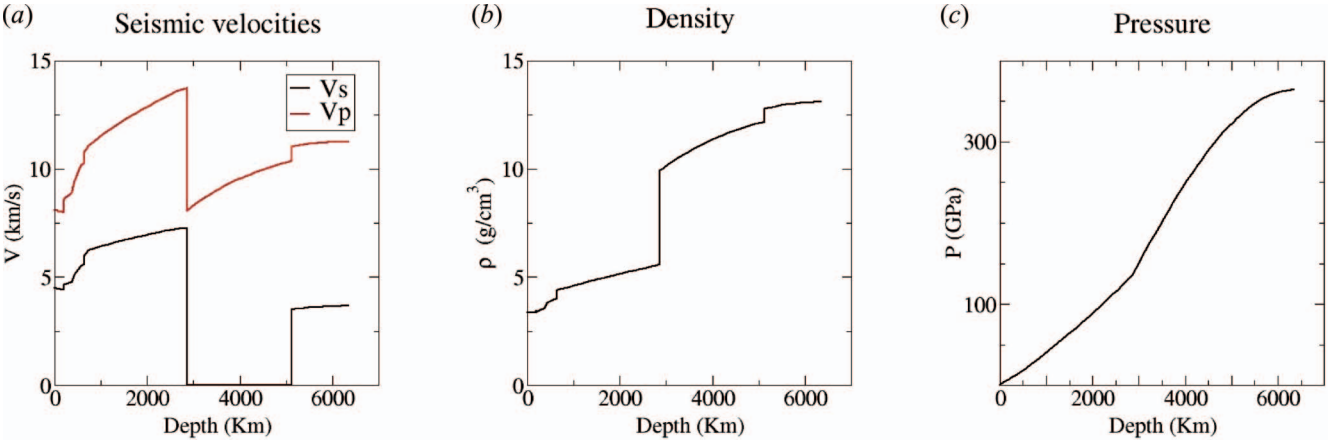

Figure 2. Structure of the Earth from seismic data: (*a*) velocities v_P and v_S of longitudinal (pressure) and transverse (shear) seismic waves, (*b*) density, and (*c*) pressure as a function of depth.

where p is pressure; the second equation follows from the first, since the variation of pressure with radius is $dp/dr = -\rho g$, with ρ the mass density and g the acceleration due to gravity at radius r; the third equation expresses the adiabatic variation of T with p in terms of the Grüneisen parameter γ and the adiabatic bulk modulus K_S. Since K_S and g can be obtained from seismic measurements, the only unknown is γ, which can be estimated from experiments [6] or, as we shall see below, from first principles calculations.

In order to integrate equation (1) one needs at least one fixed point. A long-established strategy to obtain a fixed point is to exploit the presence of the ICB, which by definition must be at the melting temperature. Since the pressure of the ICB is accurately known (329 GPa), and since the main constituent of the core is Fe, a first approximation of the temperature of the ICB can be found by measuring the melting temperature of Fe at 329 GPa.

The past couple of decades have seen strenuous efforts dedicated to the solution of the problem of determining the high pressure melting behaviour of Fe [7–17]. In particular, the only data available on the temperature of iron at core conditions are those obtained in shock wave experiments [15–17]. In these experiments a high velocity projectile is fired at the sample, and high pressure, high temperature conditions are produced upon impact. The natural outcome from these experiments is the relation between the volume and the pressure of the sample, which follows the so-called *Hugoniot* equation of state, $p(V)$. To identify melting one uses the discontinuity in the speed of sound, which can also be measured accurately, as this changes significantly when the system transforms from solid to liquid. The temperature is not readily available in these experiments, but this can be obtained by integrating an appropriate thermodynamic relation from a known starting point [16]. For this, one needs to know the Grüneisen parameter and the constant volume specific heat, which need to be estimated or, as mentioned above, calculated with the help of first principles simulations.

At lower pressure it is possible to perform diamond anvil cell experiments, in which the sample is compressed inside a pressure medium and the temperature, in principle, is directly measured. However, these experiments are not easy to perform either, and they are prone to a whole range of technical problems: for example, the pressure is deduced by the volume of the pressure medium, ruby or gold are two possibilities, but their equation of state is still being debated; the temperature is sometimes measured by fitting the electromagnetic radiation emitted by the sample to the Planck function, but this can only be done after some assumption on the emissivity of the sample as a function of the wavelength. Moreover, it was recently pointed out that chromatic effects induced by the diamond windows can be substantial, and may lead to an underestimate of melting temperatures of several hundred degrees [14]. Finally, there is the problem of identifying the correct melting transition (this problems is also present in shock wave experiments), as the possibility of confusing this with a solid–solid transition cannot be excluded. The difficulty of getting reliable and definite results for the melting curve of iron even at a pressure as low as 60 GPa is evident in the scattering of the data from different experimental groups [8–14], with differences as large as 500–1000 K on a presumed melting temperature of about 3000 K (see figure 5, section 3.3, which include some of these experimental results).

The development of theoretical methods based on the very basic laws of nature of quantum mechanics (developed 80 years ago), coupled with the recent staggering increase of computer power ($\sim$500-fold in the past 10 years), has made it possible to approach these problems from a theoretical–computational point of view. When high level first-principles methods are used, the results are often comparable in quality with experiments, sometimes even providing information in regions of the pressure–temperature space inaccessible to experiments. Here one applies the basic laws of quantum mechanics to describe the interactions between nuclei and electrons. These interactions uniquely define the *chemical potentials* of the elements involved, which completely determine the thermodynamic properties of the system, including melting temperatures. As we shall see, knowledge of the chemical potentials of different light elements in solution in Fe can also be used to put constraints on the composition of the Earth's core.

The exact quantum mechanical treatment of a system containing a large number of atoms is a formidable task. The starting point of nearly every quantum mechanical calculation is the so-called adiabatic approximation, which exploits the large difference of mass between the nuclei and the electrons. Since the electrons are much lighter, they move so much faster that on the time-scale of their movement the nuclei can be considered as fixed. Therefore one solves only the electronic problem in which the nuclei are fixed and act as an external potential for the electrons. The energy of the electrons plus the Coulomb repulsion of the nuclei, is therefore a function of the position of the nuclei, and can act as a potential energy for the nuclei. This can be mapped in configuration space to create a potential energy surface, which can later be used to study the motion of the nuclei. Alternatively, forces can be calculated as the derivatives of the potential energy with respect to the position of the nuclei, and these can be used to move the atoms around, relax the system, solve the Newton's equations of motion and perform molecular dynamics simulations, or calculate harmonic vibrational properties like phonons. The potential energy can also be differentiated with respect to the simulation cell parameters, which provides information on the stress tensor and therefore the pressure in the system. The solution of the electronic problem also provides insights into the electronic

structure of the system, which can be examined to study physical properties like bonding, charge distributions, magnetic densities, polarizabilities and so forth.

Most first-principles studies of the high pressure and temperature properties of Earth's forming materials are based on the implementation of quantum mechanics known as density functional theory (DFT). This is a technique that was introduced more than 40 years ago by Hohenberg and Kohn [18], and Kohn and Sham [19] in an attempt to simplify the calculation of the ground state properties of materials (in fact, later shown to be useful also for finite temperature properties [20]). The basic Hohenberg and Kohn idea was to map the system of interacting, correlated electrons acted on by a potential $V(\mathbf{r})$ onto a system of independent non-interacting electrons acted on by an *effective* potential $V_{\mathrm{KS}}(\mathbf{r})$, known as the Kohn–Sham potential. The price to pay for this apparent enormous simplification is a modification of the basic equations with the introduction of new terms, one of which, called exchange-correlation energy, is unfortunately unknown. However, Kohn and Sham proposed a simple form for the exchange-correlation functional, known as the local density approximation (LDA) [19], that would prove later as the insight which has made DFT so successful and so widespread today. More sophisticated exchange-correlation functionals were developed in the following decades, and are still being developed today, making DFT an evolving technique with increasingly higher accuracy. One additional attractive feature of DFT is the favourable scaling of computational effort with the size of the system. Traditional DFT techniques scale as N^3, where N is the number of electrons in the system, but large effort is being put into so-called $o(N)$ techniques, which for some materials already provide a scaling which is only directly proportional to the size of the system [21,22].

A wide range of properties of materials have already been predicted using DFT techniques, like structural and electronic properties, phase diagrams, thermoelastic properties, speed of sound, transport properties, melting, solutions and partitioning.

The limitations in accuracy due to the current state of the art of density functional theory are expected to be progressively removed, either through the formulation of new exchange-correlation functionals, or with the developments of alternative techniques. Among these dynamical mean field theory [23] and quantum Monte Carlo [24] are probably the most promising on a time-scale of 5 to 10 years.

After this introduction, the article is divided in three main sections. In the first we will briefly review the main ideas behind first-principles simulations, and in particular density functional theory and the pseudo-potential approximation. In section 3 we will try to explain how these first principles techniques can be used to calculate chemical potentials, and how these chemical potentials can be used, in particular, to calculate the melting temperature of pure Fe at ICB conditions. Finally, in section 4 we will describe how chemical potentials can be used to put constraints on the composition of the Earth's core, and to refine the temperature of the ICB.

2. First principles techniques

We begin this section by recalling the basic equation of quantum mechanics, the Schrödinger equation, which in the time-independent form is

$$\hat{H}\,\Psi = E\,\Psi, \tag{2}$$

where $\hat{H}$ is the Hamiltonian of the system, E is the total energy and Ψ is the many-body wave-function, which is a function of the coordinates of the M nuclei $\{\mathbf{R}_i\}$ and the N electrons $\{\mathbf{r}_i\} : \Psi = \Psi(\mathbf{R}_1, \mathbf{R}_2, \ldots, \mathbf{R}_M; \mathbf{r}_1, \mathbf{r}_2, \ldots, \mathbf{r}_N)$. If the system is isolated, in the non-relativistic approximation the Hamiltonian is given by

$$\begin{aligned}\hat{H}(\mathbf{R}_1, \mathbf{R}_2, \ldots, \mathbf{R}_M; \mathbf{r}_1, \mathbf{r}_2, \ldots, \mathbf{r}_N) = &-\sum_{i=1}^{M} \frac{\hbar^2}{2M_i}\nabla^2_{\mathbf{R}_i} - \sum_{i=1}^{N} \frac{\hbar^2}{2m}\nabla^2_{\mathbf{r}_i} \\ &+ \frac{1}{2}\sum_{i,j=1;i\neq j}^{M} \frac{Z_i Z_j e^2}{4\pi\epsilon_0|\mathbf{R}_i - \mathbf{R}_j|} + \frac{1}{2}\sum_{i,j=1;i\neq j}^{N} \frac{e^2}{4\pi\epsilon_0|\mathbf{r}_i - \mathbf{r}_j|} \\ &- \sum_{i=1}^{M}\sum_{j=1}^{N} \frac{Z_i e^2}{4\pi\epsilon_0|\mathbf{R}_i - \mathbf{r}_j|},\end{aligned} \tag{3}$$

where the first two terms are the kinetic energy operators for the nuclei and the electrons respectively, with $\hbar$ the Planck's constant h divided by $2\,\pi$, and M_i and m the masses of the nuclei and the electrons, respectively. The third and the fourth terms in the equation represent the Coulomb repulsive energy between the nuclei and between the electrons respectively, with Z_i the charges of the nuclei in units of e, the charge of the electron, and ϵ_0 is the dielectric constant of the vacuum. The last term of the equation represents the electrostatic interaction between the electrons and the nuclei.

The only experimental inputs in the Schrödinger equation in the non-relativistic approximation are four fundamental constants plus the mass of the nuclei. The four constants are the Plank's constant h, the charge of the electron e, the mass of the electron m and the dielectric constant of the vacuum ϵ_0.

As mentioned in the introduction, solving the Schrödinger equation is essentially impossible for any real system more complicated than the hydrogen atom, or more generally any system which contains two or more electrons, and therefore approximations are needed to make the problem manageable. The first approximation which can be introduced is the Born–Oppenheimer approximation, also called the adiabatic approximation. Here, one recognizes

that the masses of the nuclei M_i are much larger than the mass of the electron m (the lightest possible atom is the hydrogen atom, which is almost 2000 times heavier than the electron), which therefore move on a much faster timescale. This means that, without much loss of accuracy for most systems, one can separate the electronic problem from that of the nuclei, or in other words solve the Schrödinger equation for the electrons only, with the nuclei positions kept fixed. Therefore, we can rewrite equation (2) thus

$$\hat{H}(\mathbf{r}_1, \mathbf{r}_2, \ldots, \mathbf{r}_N; \{\mathbf{R}_i\})\Psi(\mathbf{r}_1, \mathbf{r}_2, \ldots, \mathbf{r}_N; \{\mathbf{R}_i\}) = E\{\mathbf{R}_i\}\Psi(\mathbf{r}_1, \mathbf{r}_2, \ldots, \mathbf{r}_N; \{\mathbf{R}_i\}), \quad (4)$$

where now the Hamiltonian depends only parametrically from the positions of the nuclei $\{\mathbf{R}_i\}$, and so do the wavefunction Ψ and the energy E. Once equation (4) is solved, the energy $E\{\mathbf{R}_i\}$ can be interpreted as a potential energy for the motion of nuclei. At high temperature (above the Debye temperature), the quantum nature of the nuclei becomes negligible, and with essentially no loss of accuracy one can treat their motion as they were classical particles. This allows one to perform molecular dynamics simulations, in which the Newton equations of motion for the nuclei are solved using the quantum mechanical forces evaluated from the derivative of $E\{\mathbf{R}_i\}$ with respect to the positions $\{\mathbf{R}_i\}$.

2.1 *Density functional theory*

Halving the difficulty of an impossible problem still leaves it impossible to solve, and it was not until the introduction of density functional theory in 1964 by Hohenberg and Kohn [18] that significant steps forward were made. We will briefly outline here the main ideas of density functional theory, for an in depth description of DFT the reader may consult the original papers or the excellent books by Parr and Wang [25] or Gross and Dreizler [26], or the recent book by Martin [27]. A simplified (almost) non-mathematical explanation of DFT has been given by one of the authors in an article in this very same journal [28].

Hohenberg and Kohn [18] proved that the external potential V_{ext} acting on the electrons is uniquely determined (up to a trivial additive constant) by the electron ground state density $n(\mathbf{r}) = \langle\Psi|\hat{n}(\mathbf{r})|\Psi\rangle = \int d\mathbf{r}_2 \ldots d\mathbf{r}_N |\Psi(\mathbf{r}, \mathbf{r}_2, \ldots, \mathbf{r}_N)|^2$, where Ψ is the ground state wave-function of the system and $\hat{n}(\mathbf{r})$ is the density operator. Here we have omitted the dependence of Ψ from the positions of the nuclei for simplicity. Since $n(\mathbf{r})$ determines also the number of electrons N, and since V_{ext} and N fix the Hamiltonian of the system, it turns out that the electron density completely determines all the electronic ground state properties of the system, and in fact, as shown later by Mermim [20], also the finite temperature properties. One important property of the system is the energy, which can be written as

$$E[n] = F_{\text{HK}}[n] + \int V_{\text{ext}}(\mathbf{r})n(\mathbf{r})\, \mathrm{d}\mathbf{r}, \quad (5)$$

with

$$F_{\text{HK}}[n] = \langle\Psi[n]|\hat{T} + \hat{V}_{\text{ee}}|\Psi[n]\rangle, \quad (6)$$

where $\hat{T}$ and $\hat{V}_{\text{ee}}$ are, respectively, the kinetic energy and the electron–electron interaction operators, and $\Psi[n]$ is the ground state wave-function of the system. The quantities $E[n]$ and $F_{\text{HK}}[n]$ are *functionals* of the density n, i.e. they represent a number which depends on the whole density n. Note that $F_{\text{HK}}[n]$ does not depend on the external potential and therefore it is a universal functional. This is the crucial result of DFT. Using the variational principle Hohenberg and Kohn also proved that the ground state density of the system is the one which minimizes $E[n]$, and the minimum of $E[n]$ is equal to the ground state energy E_0. It is clear the importance of these two results, the only quantity which is needed is the electron density, no matter how many electrons are present in the system.

One year after the publication of the Hohenberg and Kohn paper Kohn and Sham invented an indirect method to solve the problem [19]. The idea is to write the energy functional as an easy part plus a difficult part.

$$F[n] = T_0[n] + E_{\text{H}}[n] + E_{\text{xc}}[n], \quad (7)$$

where $T_0[n]$ is the ground state kinetic energy of an auxiliary non-interacting system whose density is the same as the one of the real system, $E_{\text{H}}[n]$ is the repulsive electrostatic energy of the classical charge distribution $n(\mathbf{r})$ and $E_{\text{xc}}[n]$ is the exchange-correlation energy defined through equation (7).

Minimizing the total energy $E[n]$ under the constraints of orthonormality for the one-particle orbitals of the auxiliary system, $\int \psi_i^*(\mathbf{r})\psi_j(\mathbf{r})\, \mathrm{d}\mathbf{r} = \delta_{ij}$, one finds a set of one-particle Schrödinger-like equations:

$$\left[-\frac{\hbar^2}{2m}\nabla^2 + V_{\text{KS}}(\mathbf{r})\right]\psi_i(\mathbf{r}) = \epsilon_i\psi_i(\mathbf{r}), \quad (8)$$

where the Kohn and Sham potential is

$$V_{\text{KS}}(\mathbf{r}) = V_{\text{ext}}(\mathbf{r}) + \int \frac{n(\mathbf{r}')}{|\mathbf{r} - \mathbf{r}'|}\, \mathrm{d}\mathbf{r}' + V_{\text{xc}}(\mathbf{r}); \quad V_{\text{xc}}(\mathbf{r}) = \frac{\delta E_{\text{xc}}[n]}{\delta n(\mathbf{r})}, \quad (9)$$

and

$$n(\mathbf{r}) = \sum_i f(\epsilon_i - \epsilon_{\text{F}})|\psi_i(\mathbf{r})|^2, \quad (10)$$

with $f(x)$ the Fermi–Dirac distribution and ϵ_F the Fermi energy fixed by the condition

$$\int n(\mathbf{r})\ \mathrm{d}\mathbf{r} = N. \tag{11}$$

Here $\delta E_{xc}[n]/\delta n(\mathbf{r})$ is the functional derivative of the exchange-correlation functional evaluated at position $\mathbf{r}$. This represents the variation of the functional $E_{xc}[n]$ with respect to a variation of the charge density n at position $\mathbf{r}$.

These are the famous Kohn and Sham equations, they must be solved self-consistently because V_{KS} is a functional of the orbitals itself. The generalization to finite temperature is obtained by replacing E with the electronic free energy $U = E - TS$, where S is the electronic entropy, given by the independent-electron formula $S = -2\ k_B\ T\ \Sigma_i[f_i \ln f_i + (1-f_i) \ln (1-f_i)]$, with f_i the thermal (Fermi–Dirac) occupation number of orbital i.

It is tempting to identify the single particle eigenvalues ϵ_i with the energy of quasi-particles, and therefore their distribution with the electronic density of states of the system. This would be conceptually wrong, as the Kohn and Sham eigenvalues are only an artificial mathematical tool to obtain at the ground state density of the system. Nevertheless, it turns out that these DFT density of states often resemble very accurately the real density of states of systems, and they are therefore often used to analyse their electronic structure. However, it is important to remember that even if the exact exchange-correlation functional $E_{xc}[n]$ were known, one should not expect the DFT density of states to be an exact representation of the real density of states of the system.

When self-consistency is achieved the electronic free energy of the system is

$$U = \sum_{i=1}^{N} f(\epsilon_i - \epsilon_F)\epsilon_i - \frac{1}{2}\int \frac{n(\mathbf{r})n(\mathbf{r}')}{|\mathbf{r}-\mathbf{r}'|}\ \mathrm{d}\mathbf{r} + E_{xc}[n] - \int V_{xc}(\mathbf{r})n(\mathbf{r})\ \mathrm{d}\mathbf{r} + E^{ion} - TS, \tag{12}$$

where E^{ion} is the ionic electrostatic repulsion term. This would be the exact electronic free energy of the system if we knew $E_{xc}[n]$ (which also depends on temperature, although very little is known about this dependence). Unfortunately the exact form of the exchange-correlation (free) energy is not (yet) known.

2.1.1. Exchange correlation functionals. Kohn and Sham [19] also provided an approximate expression for the exchange-correlation functional, called the Local Density Approximation (LDA). In the LDA the dependence of the functional on the density has the form

$$E_{xc}^{LDA}[n] = \int n(\mathbf{r})\epsilon_{xc}(n(\mathbf{r}))\ \mathrm{d}\mathbf{r}, \tag{13}$$

and $\epsilon_{xc}(n)$ is taken to be the exchange-correlation energy per particle of a uniform electron gas whose density is $n(\mathbf{r})$. This has been accurately calculated using Monte Carlo simulations [29] and parameterized in order to be given in an analytic form [30].

By construction, this approximation yields exact results if the density of the system is uniform, and should not be very accurate for those systems whose density is highly dishomogeneous, as for example atoms and molecules. However, it turns out to work better than expected for a wide range of materials. In molecules, for example, the LDA usually overestimates the binding energies, but it yields in general good results for equilibrium distances and vibrational frequencies. It was the evidence of the very high quality of the LDA that has been mainly responsible for the tremendous success of density functional theory.

Nowadays, a number of sophisticated functionals have become available, like the so-called generalized gradient corrections (GGA) (e.g. [31]), or the recently developed metaGGA [32,33], and hybrid functionals which contain a certain fraction of exact exchange according to various recipes (e.g. the B3LYP functional [34]), but it is not obvious which one to prefer in general, with the good old LDA itself being competitive in accuracy in a variety of cases. It is also worth mentioning that, when used in combination with plane-waves methods (see next section), exchange-correlation hybrid functionals usually require a computational effort that is orders of magnitudes higher than what is required by local exchange-correlation functionals like the LDA or the GGAs.

Whatever functional is used, these type of calculations all go under the classification of *ab initio*, in the sense that no experimental input is allowed, a part from the four fundamental constants mentioned above. Of course, it would be desirable to have a unique functional with the highest possible accuracy for any system, but at the time of writing we are not at this stage yet.

2.1.2. Pseudo-potentials and basis sets. In practical cases, it is often necessary to introduce one additional approximation in order to speed up the calculations, known as the *pseudo-potential* approximation [35–37]. In essence, this is a way to freeze the electrons of the core of the atoms, and remove them from the calculations. The justification for doing this is that the core electrons are so tightly bound to the nuclei that they are essentially undisturbed by the chemical bonding, or, conversely, the chemistry of materials is unaffected by the behaviour of the core electrons. This implies a saving in complexity and computer time which is proportional to the number of electrons that have been frozen, but as we shall see in a moment, the saving becomes enormous in the most widely diffused computer codes which are based on plane wave expansions of the single particle Kohn and Sham orbitals.

In order to solve the Kohn and Sham equations, it is necessary to expand the auxiliary Kohn and Sham orbitals in terms of some known basis functions. A variety of possible choices are available. Traditional quantum chemistry codes often use gaussians, which are quite well suited for very localized orbitals, and in the course of the years a large amount of expertise has been accumulated to create high quality basis sets for a wide range of materials. The drawback of gaussians is that the quality of the basis set depends on the choices of the user, and transferability can be an issue when different systems are compared. An alternative set of functions which are totally unbiased and systematically improvable are plane waves. They also have the additional advantage that they adapt naturally to calculations in which periodically boundary conditions are employed, which is a very useful set-up even in a system which has no periodicity, in order to reduce finite size effects. Plane wave calculations are relatively simple, and the evaluation of forces and the stress tensor are not much more difficult than the evaluation of the total energy. A drawback of plane waves is that a large number of them may be needed for describing rapidly varying functions, like the very localized core orbitals, or the valence wave-functions in the core region which need to oscillate widely in order to be orthogonal to the core orbitals. For this reason plane-wave calculations are almost always associated with the use of pseudo-potentials.

The first aim of pseudo-potentials is to eliminate the core electrons from the explicit calculations because they do not participate in the chemical properties of matter, at least until their binding energy is much higher than the energy involved in the chemical properties one wants to study. So one freezes them around the nuclei and redefines the system as if it was formed by ions plus valence electrons. We are left now with the problem of dealing with the oscillations in the core region of the valence wave-functions, due to the orthogonalization to the core wave-functions. The solution to this is the introduction of a pseudo-potential, which substitutes the ionic Coulomb potential in such a way that: (i) the valence pseudo-eigenvalues are the same as the all-electron ones on some reference configuration in the atom; (ii) the pseudo-wave-functions coincide with the all-electron ones from a fixed core radius on, and are as smooth as possible below the core radius, with the only constraint to be normalized (norm-conserving pseudo-potentials). To satisfy these requirements the pseudo-potential usually must be angular momentum dependent, i.e. pseudo-wave-functions corresponding to different angular momenta are eigenfunctions of different potentials. However, the long-range behaviour of these different potentials must resemble the true one, because above the core radius the pseudo-wave-functions are identical to the all-electron ones. This mean that the difference must be confined in the core region. The quality of the pseudo-potential depends on its transferability properties, i.e. the capability to reproduce the all-electron results over a wide range of electronic configurations, and of course for the atom in different environments.

2.1.3. Ultra-soft (Vanderbilt) pseudo-potentials. The requirement of norm conservation for the pseudo-wave-functions can be a limiting factor for numerical calculations when also the valence electrons are very localized around their nuclei. This is a particularly serious problem for first row elements, like carbon and more so for nitrogen, oxygen, and for transition metals, where the *d*-electrons are localized as shallow core states but have an extraction energy which is not much larger then valence energies, and for this reason cannot be excluded from the calculations. Iron for example is one of these elements. If this is the case the utilization of norm-conserving pseudo-potentials requires huge plane-waves basis sets to achieve an acceptable accuracy. In a work published in 1990 Vanderbilt [38] showed that, introducing a generalized formalism, the norm conservation constraint could be removed. In this way one can construct much smoother pseudo-wave-functions, with the only constraint of matching the all-electron ones at and above a fixed core radius. The price to pay for having such smooth pseudo-wave-functions is that, due to the fact that the pseudo-wave-functions are not normalized anymore, the charge density has to be restored by adding an 'augmentation' part:

$$n(\mathbf{r}) = \sum_i |\phi_i(\mathbf{r})|^2 + n_{\text{aug}}(\mathbf{r}), \tag{14}$$

and the Kohn and Sham equations take the generalized form

$$H_{\text{KS}}|\phi_i\rangle = \epsilon_i S|\phi_i\rangle, \tag{15}$$

where S is a non-local overlap operator.

2.1.4. The projector augmented wave method. In 1994 Blöchl invented a method to reconstruct the all-electron wave-function inside the core region [39]. The method, called Projected Augmented Wave (PAW), is closely related to Vanderbilt's Ultrasolf Pseusopotential method, as shown by Kresse and Joubert [40], but has been shown to be capable of reproducing essentially the same results of all-electron calculations, effectively removing the pseudo-potential approximation. The PAW method is still only available in a handful of computer codes, but as evidence of its advantages accumulate it is likely that it will become a standard method for DFT-plane-waves calculations.

3. Melting of Fe at Earth's core conditions

Having introduced the main computational tools we now turn the discussion to the two main topics of this article, namely the calculation of the iron melting curve at Earth's core conditions in this section, and the constraints on the composition of the Earth's core in the next section. The reason why we begin with the melting of Fe will become clear as we proceed. This has to do with the fact that the technique to put constraints on the composition of the Earth's core builds on previous knowledge of the thermodynamic properties of pure iron at the melting point.

All the calculations described in this article have been performed with the code VASP [41].

The thermodynamic stability of a system is determined by the minimum of its Gibbs free energy $G = F + pV$, where F is the Helmholtz free energy, p is the pressure in the system, given by $p = -\partial F/\partial V|_T$ and V is the volume. Below the melting temperature the system is solid, and therefore the Gibbs free energy of the solid is lower than that of the liquid. The converse happens above the melting temperature, where the system is liquid. Therefore, the thermodynamic condition at which a solid coexists with its liquid at pressure p and temperature T is determined by the equality:

$$G_s(p, T) = G_l(p, T), \tag{16}$$

where subscripts 's' and 'l' indicate solid and liquid, respectively.

The condition stated in equation (16) gives us a strategy to obtain the melting temperature of Fe at any pressure, provided we can calculate the Gibbs free energies of solid and liquid as a function of pressure and temperature (see figure 3). Since $G = F + pV$ it is possible to calculate G from knowledge of F. In the following we now describe how this can be done.

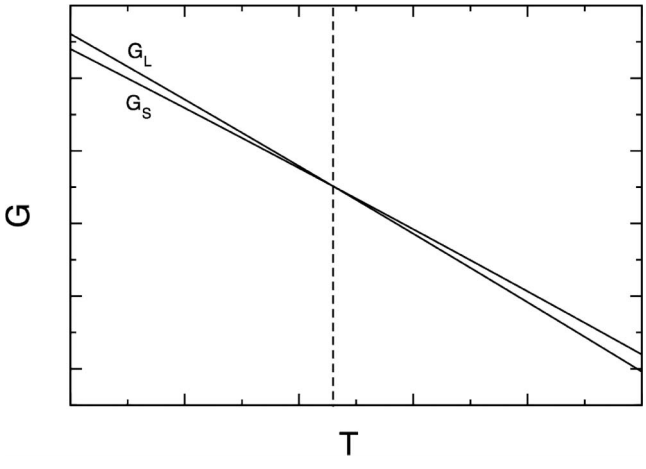

Figure 3. Schematic plot of Gibbs free energies G_S and G_L of solid and liquid as a function of temperature at fixed pressure, to illustrate procedure for determining melting temperature.

3.1 *The Helmholtz free energy: low temperature and the quasi-harmonic approximation*

For solids at not too high a temperature, it is often accurate enough to use the *quasi-harmonic approximation*, in which the potential energy of the crystal is expanded to second order in the displacement of the atoms from their equilibrium positions. This quasi-harmonic potential usually provides a very accurate description of the dynamical properties of the system at low temperature, and gives easy access to the free energy of the system, which can be calculated analytically as a function of temperature. The prefix quasi is there to indicate that this quasi-harmonic potential depends on the volume of the system. In practice, the quality of the thermodynamics obtained within the quasi-harmonic approximation is often preserved also to temperatures not far from the melting temperature, although at such high temperatures a full account of anharmonic effects becomes necessary, at least to asses the validity of the quasi-harmonic approximation. For highly anharmonic solids and for liquids one has to resort to molecular dynamics or Monte Carlo techniques to sample the phase space. Molecular dynamics simulations are particularly attractive because they also provide dynamical information like diffusion. We shall come back to this in the next subsection.

In a perfect crystal the quasi-harmonic approximation is obtained by expanding the potential (free) energy function U around the equilibrium positions of the nuclei. The first term of the expansion is simply the energy of the system calculated with the ions in their equilibrium positions, $E_{\mathrm{perf}}(V, T)$ (this is a free energy at finite temperature due to electronic excitations, and therefore depends both on V and T). If the crystal is in its minimum energy configuration the linear term of the expansion is zero, and by neglecting terms of order three and above in the atomic displacements we have that the quasi-harmonic potential is

$$U_{\mathrm{harm}} = E_{\mathrm{perf}} + \frac{1}{2}\sum_{ls\alpha, l't\beta} \Phi_{ls\alpha, l't\beta} u_{ls\alpha} u_{l't\beta}, \tag{17}$$

where $\mathbf{u}_{ls}$ denotes the displacement of atom s in unit cell l, α and β are Cartesian components, and $\Phi_{ls\alpha,\ l't\beta}$ is the force-constant matrix, given by the double derivative $\partial^2 U/\partial u_{ls\alpha}\partial u_{l't\beta}$ evaluated with all atoms at their equilibrium positions. This force constant matrix gives the relation between the forces $\mathbf{F}_{ls}$ and the displacements $\mathbf{u}_{l't}$, as can be seen by differentiating equation (17) and ignoring the higher-order anharmonic terms:

$$F_{ls\alpha} = -\partial U/\partial u_{ls\alpha} = -\sum_{l't\beta} \Phi_{ls\alpha, l't\beta} u_{l't\beta}. \tag{18}$$

Within the quasi-harmonic approximation, the potential energy function $U_{\rm harm}$ completely determines the physical properties of the system, and in particular the Helmholtz free energy, which takes the form

$$F(V,T) = E_{\rm perf}(V,T) + F_{\rm harm}(V,T), \qquad (19)$$

where the quasi-harmonic component of the free energy is

$$F_{\rm harm} = k_{\rm B}T \sum_n \ln\,(2\,\sinh\,(\hbar\omega_n/2k_{\rm B}T)), \qquad (20)$$

with ω_n the frequency of the nth vibrational mode of the crystal. In a periodic crystal, the vibrational modes can be characterized by a wave-vector $\mathbf{k}$, and for each such wave-vector there are three vibrational modes for every atom in the primitive cell. If the frequency of the sth mode at wave-vector $\mathbf{k}$ is denoted by $\omega_{\mathbf{k}s}$, then the vibrational free energy is

$$F_{\rm harm} = k_{\rm B}T \sum_{\mathbf{k}s} \ln\,(2\,\sinh\,(\hbar\omega_{\mathbf{k}s}/2k_{\rm B}T)). \qquad (21)$$

The vibrational frequencies $\omega_{\mathbf{k}s}$ can be calculated from first principles, and we shall see below how this can be done.

Once this quasi-harmonic free energy is known, all the thermodynamic properties of the system can be calculated. In particular, the pressure is given by

$$p = -\partial F/\partial V|_T = -\partial E_{\rm perf}/\partial V|_T - \partial F_{\rm harm}/\partial V|_T. \qquad (22)$$

The last term in the equation above is the ionic component of the thermal pressure, and it is different from zero because the vibrational frequencies $\omega_{\mathbf{k}}s$ depend on the volume of the crystal. In fact, it is easy to see from equation (21) that even at zero temperature there is a finite contribution to the quasi-harmonic free energy, given by

$$F_{\rm harm}(V,0) = \sum_{\mathbf{k}s} \frac{\hbar\omega_{\mathbf{k}s}}{2}. \qquad (23)$$

This zero point energy contribution to the harmonic free energy is also responsible for a contribution to the pressure. Since usually the vibrational frequencies $\omega_{\mathbf{k}}s$ increase with decreasing volume, these contributions are positive, and are responsible for the phenomenon of thermal expansion in solids.

The dependence of $E_{\rm perf}\,(V,\,T)$ on T also means that there is an electronic contribution to the thermal pressure, which is also positive, and in some cases (i.e. iron at Earth's core conditions) can be a significant fraction of the thermal pressure, and a non-negligible fraction of the total pressure [42].

We will now describe how the vibrational frequencies $\omega_{\mathbf{k}}s$ can be calculated.

3.1.1. Calculation of phonon frequencies. There are two different first-principles strategies for calculating phonon frequencies. The method that is easier to understand starts from the fact that the force-constant matrix expresses the proportionality between displacements and forces, when the displacements are small enough for this relationship to be linear (see equation (18)). All that has to be done in principle is to displace a single atom t in cell l' in Cartesian direction β, all other atoms being held fixed at their equilibrium positions; the forces $F_{ls\ \alpha}$ on all the atoms then give directly the elements of the force constant matrix $\Phi_{ls\alpha,l't\beta}$ for the given ($l'\ t\beta$). If this procedure is repeated for all other ($l't\beta$), all the elements of the force-constant matrix can be obtained. Translational invariance implies that the number of separate calculations required to do this is at most three times the number of atoms in the primitive cell, but for most materials symmetry relations can be used to reduce this number substantially. This strategy, sometimes called the small displacement method [43], is implemented for example in the PHON code [44]. Although the small displacement method is widely used, and can be very accurate, a word of caution is in order. Since DFT calculations on condensed matter always use periodic boundary conditions, the repeating cell (the *super-cell*) must be large enough so that the elements $\Phi_{ls\alpha,l't\beta}$ have all fallen off to negligible values at the boundary of the super-cell. This is readily achieved for some materials, particularly metals. However, in ionic materials the force constant elements fall off only as r^{-3}, and convergence can be slow. Moreover, in polar materials Coulomb forces produce a macroscopic electric field in the limit of zero wave-vector. This electric field is responsible for a splitting in the frequencies of the vibrational modes parallel and perpendicular to the electric field (the so-called LO-TO splitting). It turns out that the behaviour of the dynamical matrix in the limit of small wave-vector is non-analytical, and has the following form [45]

$$D^{\rm na}_{s\alpha,t\beta} = (m_s m_t)^{-1/2} \frac{4\pi e^2}{\Omega} \frac{(\mathbf{k}\cdot\mathbf{Z}^*_s)_\alpha (\mathbf{k}\cdot\mathbf{Z}^*_t)_\beta}{\mathbf{k}\cdot\epsilon^\infty\cdot\mathbf{k}}, \qquad (24)$$

where $\mathbf{Z}^*_s$ is the Born effective charge tensor for atom s, ϵ^∞ is the high frequency static dielectric tensor and m_s, m_t are the mass of the atoms. These two quantities can be calculated in the framework of density functional perturbation theory [45–47] (DFPT), which also provides a second elegant strategy for the calculation of phonons in crystals. The main idea in DFPT, pioneered by Baroni *et al*. [46] is to exploit the Hellmann–Feynman theorem to show that a linear order variation in the electron density upon application of a perturbation to the crystal is responsible for a variation in the energy up to second (in fact, third [48]) order of the perturbation. Using standard perturbation theory, this linear order variation of the electronic charge density can be calculated using only unperturbed wave-functions, which therefore only require calculations

on the ground state crystal. If the perturbation is a phonon wave with wave-vector **k**, calculation of the density change to linear order in the perturbation can be used to determine the force constant matrix at wave-vector **k**. This can be done for any arbitrary wave-vector, without the need of the construction of a super-cell. The implementation of the method is by no means straightforward, and for further details the reader should consult the original papers [45,46].

For Fe the small displacement method [44] works very well, and only super-cells of modest size (36 atoms) are necessary to obtain free energies accurate enough so that their contribution to the error in the melting temperature is no more than a few tens of K.

As a matter of illustration of the accuracy of these first principles techniques in describing the vibrational properties of Fe we show in figure 4 the phonon curves of ferromagnetic Fe from GGA calculations [49] compared with experimental results, which show a very satisfactory agreement.

3.2 *The Helmholtz free energy: high temperature and thermodynamic integration*

At high temperature anharmonic effects in solids may start to play an important role, and the quasi-harmonic approximation may not be accurate enough. Moreover, if the system of interest is a liquid, the quasi-harmonic approximation is of no use. In this section we shall describe a method to calculate the free energy of solids and liquid in the high temperature limit, provided that the temperature is high enough that the quantum nature of the nuclei can be neglected. If this is the case, the Helmholtz free energy F is defined as [50]:

$$F = -k_{\mathrm{B}}T \ln \left\{ \frac{1}{N!\Lambda^{3N}} \int_V \mathrm{d}\mathbf{R}_1 \ldots \mathrm{d}\mathbf{R}_N \times \exp\left[-\beta U(\mathbf{R}_1, \ldots, \mathbf{R}_N; T)\right] \right\}, \tag{25}$$

where $\Lambda = h/(2\pi M k_{\mathrm{B}}T)^{1/2}$ is the thermal wavelength, with M the mass of the particles, h Plank's constant, $\beta = 1/k_{\mathrm{B}}T$, k_{B} is the Boltzmann constant, and $U(\mathbf{R}_1, \ldots, \mathbf{R}_N; T)$ is the potential energy function, which depends on the positions of the N particles in the system and on temperature because of electronic excitations. The multidimensional integral extends over the total volume of the system V.

Performing the integral in equation (25) to calculate F is extremely difficult. However, it is less difficult to calculate changes in F as some specific variables are changed in the system. For example, by taking the derivative of F in equation (25) with respect to volume at constant T we obtain (minus) the pressure. Therefore, the difference of F between two volumes can be obtained by integrating the pressure p, which can be calculated using a *molecular dynamics simulation* [50]. Similarly, by integrating the internal energy E one obtains differences in F/T.

It is equally possible to calculate differences in free energy between two systems having the same number of atoms N, the same volume V, but two different potential energy functions U_0 and U_1. This can be done by introducing an intermediate potential energy function U_λ such that for $\lambda = 0$; $U_\lambda = U_0$, and for $\lambda = 1$; $U_\lambda = U_1$, and such that for any value of $0 < \lambda < 1$, U_λ is a continuous and differentiable function of λ. For example, a convenient form is

$$U_\lambda = (1 - f(\lambda))U_0 + f(\lambda)U, \tag{26}$$

where $f(\lambda)$ is an arbitrary continuous and differentiable function of λ in the interval $0 \le \lambda \le 1$, with the property $f(0) = 0$ and $f(1) = 1$. According to equation (25), the Helmholtz free energy of this intermediate system is

$$F_\lambda = -k_{\mathrm{B}}T \ln \left\{ \frac{1}{N!\Lambda^{3N}} \int_V \mathrm{d}\mathbf{R}_1 \ldots \mathrm{d}\mathbf{R}_N \times \exp\left[-\beta U_\lambda(\mathbf{R}_1, \ldots, \mathbf{R}_N; T)\right] \right\}. \tag{27}$$

Differentiating this with respect to λ gives

$$\frac{\mathrm{d}F_\lambda}{\mathrm{d}\lambda} = \frac{\int_V \mathrm{d}\mathbf{R}_1 \ldots \mathrm{d}\mathbf{R}_N \exp\left[-\beta U_\lambda(\mathbf{R}_1, \ldots \mathbf{R}_N; T)\right](\partial U_\lambda/\partial\lambda)}{\int_V \mathrm{d}\mathbf{R}_1 \ldots \mathrm{d}\mathbf{R}_N \exp\left[-\beta U_\lambda(\mathbf{R}_1, \ldots \mathbf{R}_N; T)\right]} = \left\langle \frac{\partial U_\lambda}{\partial\lambda} \right\rangle_\lambda, \tag{28}$$

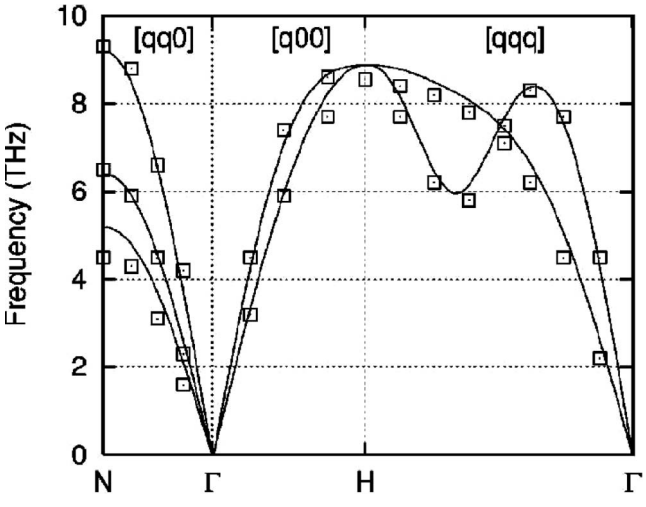

Figure 4. Phonon dispersion relations of ferromagnetic bcc Fe. Lines and open squares show first-principles theory and experiment, respectively. Symbols Γ, H and N represent special points in the Brillouin zone. Reproduced with permission from [49]. Copyright 2000 American Physical Society.

and therefore by integrating dF_λ/d_λ one obtains

$$\Delta F = F_1 - F_0 = \int_0^1 d\lambda \left\langle \frac{\partial U_\lambda}{\partial \lambda} \right\rangle_\lambda . \quad (29)$$

This also represents the reversible work done on the system as the potential energy function is switched from U_0 to U_1. In most cases a suitable choice for the function that mixes U_0 and U_1 is simply $f(\lambda) = \lambda$, and the thermodynamic formula (29) takes the simple form:

$$\Delta F = F_1 - F_0 = \int_0^1 d\lambda \langle U_1 - U_0 \rangle_\lambda . \quad (30)$$

This way to calculate free energy differences between two systems is called *thermodynamic integration* [50]. The usefulness of the thermodynamic integration formula expressed in equation (29) becomes clear when one identifies U_1 with the DFT potential (free) energy function, and with U_0 some classical model potential for which the free energy is easily calculated, to be taken as a reference system. Then equation (29) can be used to calculate the DFT free energy of the system by evaluating the integrand $\langle U_1 - U_0 \rangle_\lambda$ using *first principles molecular dynamics* simulations at a sufficiently large number of values of λ and calculating the integral numerically.

Thermodynamic integration can be used to calculate the free energies of both solids and liquids. It is clear from equation (29) that the choice of the reference system is almost completely irrelevant (of course, the stability of the system cannot change as λ is switched from 0 to 1), provided that ΔF can be calculated in practice. So, if the goal is to obtain *ab initio* free energies, it is essential to minimize the amount of *ab initio* work in order to make the calculations feasible. This is achieved by requiring that: (i) the integrand in equation (29) is a smooth function of λ, (ii) the thermal averages $\langle U_1 - U_0 \rangle_\lambda$ can be computed within the required accuracy on the time-scales accessible to first principles molecular dynamics and (iii) the convergence of ΔF as a function of the number of atoms N in the system is again achieved with N accessible to first-principles calculations.

In high pressure high temperature Fe it turns our that a remarkably good reference potential is given by a simple inverse power model of the form $U_{IP}(r) = B/r^\alpha$, where r is the distance between two ions and B and α are two adjustable parameters appropriately chosen. The parameter α turns out to be slightly less than 6, which indicates that under these extreme conditions Fe behaves like an ensemble of soft spheres.

3.3 *Melting curve of Fe*

Once the Helmholtz free energy of the system is known, it can be used to derive its thermodynamic properties, and in particular its melting curve. So, we obtain the Gibbs free energy from the Helmholtz free energy, and we apply equation (16) to obtain the melting curve of Fe. This can be done in a whole range of pressure spanning the Earth's core, and the results are shown in figure 5, where an error band of about plus or minus 600 K has to be added to the calculated melting curve. For a more in depth discussion of the technical points in these calculations we refer the reader to the original papers [42,51–53]. We also show on the figure a number of experimental points. In the low pressure region these are diamond anvil cell experiments, while in the high pressure region they correspond to shock experiments. The scattering between these points reminds us how difficult it is to perform these experiments. The theoretical predictions are in good agreement with the shock data experiments [16,17] and with some late diamond anvil cell experiments [13].

4. Constraints on the composition of the Earth's core

We can now turn the discussion to the topic of the composition of the Earth's core. It will be shown that by combining first principles calculations of free energies, or more precisely *chemical potentials*, with seismic data, it is possible to put constraints on the composition of the core. In particular, we shall show that no binary mixture of Fe/S, Fe/Si or Fe/O can explain the seismic data, and we propose an Earth's core composition based on ternary and

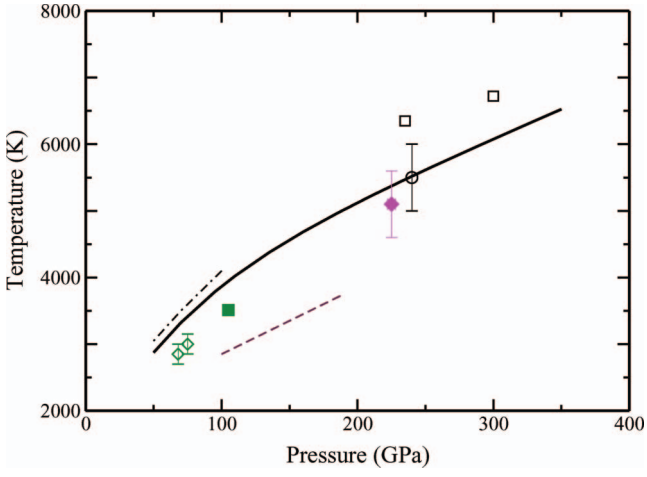

Figure 5. Comparison of melting curve of Fe from DFT calculations and experimental data: black solid first-principles results of [51] (plus or minus 600 K); black chained and maroon dashed curves: diamond anvil cell measurements of [8,11]; green diamonds and green filled square: diamond anvil cell measurements of [10,13]; black open squares, black open circle and magenta diamond: shock experiments of [15]. Error bars are those quoted in original references.

quaternary mixtures of Fe with all three light elements considered. In the discussion we will ignore the presence of Ni in the core, which we believe should not influence the results and the final conclusions significantly. The most important results from our discussion will be that oxygen almost completely partitions in the liquid, and therefore is expelled by the mixture as this freezes at the inner core boundary. The availability of light buoyant oxygen at the bottom of the liquid core is a source of gravitational energy, which can be efficiently used to produce the *geodynamo* and the resulting Earth's magnetic field.

4.1 *Solutions*

Consider two different substances, mix them together and in general they will form a solution, like sugar and coffee. We call solvent the substance present in the largest quantity (coffee), and solute the other (sugar). In general solutions may have more than one solute, and/or more than one solvent, but for simplicity we will focus here only on binary mixtures.

We mentioned at the beginning of the previous section that the phase stability of a system is determined by the minimum of its Gibbs free energy. More generally, equilibrium in a multi-species system is determined by the chemical potentials μ_i, with i running over the different species, which represents the constant of proportionality between the energy of the system and the amount of the specie i [54]:

$$\mu_i = \left(\frac{\partial E}{\partial N_i}\right)_{S,V}, \tag{31}$$

where S is the entropy, and N_i is the number of particles of the specie i. Alternative equivalent definitions of the chemical potential are [54,55]:

$$\mu_i = \left(\frac{\partial F}{\partial N_i}\right)_{T,V} = \left(\frac{\partial G}{\partial N_i}\right)_{T,p} = -T\left(\frac{\partial S}{\partial N_i}\right)_{E,V}. \tag{32}$$

Equilibrium between two phases is determined by the condition of equality of the chemical potential of each individual specie in the two phases, as we shall see in the next subsection.

4.1.1. Solid liquid equilibrium. We want to study now the conditions that determine equilibrium between solid and liquid, and in particular how the solute partitions between the two phases and how this partitioning affects the melting properties of the solution. This will allow us to interpret the seismic data at the ICB, which is the place where a liquid mixture of Fe with light impurities coexists with a solid mixture.

Thermodynamic equilibrium is reached when the Gibbs free energy of the system is at its minimum, and therefore $0 = \mathrm{d}G = \mathrm{d}(G^{\mathrm{l}} + G^{\mathrm{s}})$, where superscripts 's' and 'l' indicate quantities in the solid and in the liquid, respectively. In a multicomponent system the Gibbs free energy can be expressed in terms of the chemical potentials of the species present in the system [54,55]:

$$G = \sum_i N_i \mu_i. \tag{33}$$

We also recall the Gibbs–Duhem equation, which relates the changes in the chemical potentials of the various components in the system and their amount [54]:

$$\sum_i N_i \, \mathrm{d}\mu_i = 0. \tag{34}$$

Using equation (33) and the Gibbs–Duhem equation (34), we obtain

$$\mathrm{d}G = \sum_i \mu_i \, \mathrm{d}N_i. \tag{35}$$

If the system is isolated, particles can only flow between the solid and the liquid, and we have $\mathrm{d}N_i^{\mathrm{s}} = -\mathrm{d}N_i^{\mathrm{l}}$, which implies

$$\mathrm{d}G = \sum_i \mathrm{d}N_i(\mu_i^{\mathrm{l}} - \mu_i^{\mathrm{s}}). \tag{36}$$

If $\mu_i^{\mathrm{l}} < \mu_i^{\mathrm{s}}$ there will be a flow of particles from the solid to the liquid region ($\mathrm{d}N_i > 0$), so that the Gibbs free energy of the system is lowered. The opposite will happen if $\mu_i^{\mathrm{l}} > \mu_i^{\mathrm{s}}$. The flow stops at equilibrium, which is therefore reached when $\mu_i^{\mathrm{l}} = \mu_i^{\mathrm{s}}$. In particular, in our two components system, equilibrium between solid and liquid implies that the chemical potentials of both solvent and solute are equal in the solid and liquid phases:

$$\begin{aligned} \mu_{\mathrm{X}}^{\mathrm{s}}(p, T_{\mathrm{m}}, c_{\mathrm{X}}^{\mathrm{s}}) &= \mu_{\mathrm{X}}^{\mathrm{l}}(p, T_{\mathrm{m}}, c_{\mathrm{X}}^{\mathrm{l}}); \\ \mu_{\mathrm{A}}^{\mathrm{s}}(p, T_{\mathrm{m}}, c_{\mathrm{X}}^{\mathrm{s}}) &= \mu_{\mathrm{A}}^{\mathrm{l}}(p, T_{\mathrm{m}}, c_{\mathrm{X}}^{\mathrm{l}}); \end{aligned} \tag{37}$$

where T_{m} is the melting temperature of the solution at pressure p. As the concentration of the solute is reduced the number of ways it can be arranged in the solvent increases, and therefore the entropy increases. In the limit of zero concentration the entropy diverges, which causes a divergence in the chemical potential. This is a logarithmic divergence and can be separated out, and the chemical potential can be conveniently rewritten as

$$\mu = k_{\mathrm{B}} T \ \ln \ c + \tilde{\mu}(p, T, c), \tag{38}$$

where $\tilde{\mu}(p, T, c)$ is a well behaved function of concentration c. We can now use this expression to rewrite the first of the two equations above as

$$\begin{aligned} &\tilde{\mu}_{\mathrm{X}}^{\mathrm{s}}(p, T_{\mathrm{m}}, c_{\mathrm{X}}^{\mathrm{s}}) + k_{\mathrm{B}} T_{\mathrm{m}} \ \ln \ c_{\mathrm{X}}^{\mathrm{s}} \\ &\quad = \tilde{\mu}_{\mathrm{X}}^{\mathrm{l}}(p, T_{\mathrm{m}}, c_{\mathrm{X}}^{\mathrm{l}}) + k_{\mathrm{B}} T_{\mathrm{m}} \ \ln \ c_{\mathrm{X}}^{\mathrm{l}}. \end{aligned} \tag{39}$$

From which we obtain an expression for the ratio of concentrations of solute between the solid and the liquid:

$$c_{\mathrm{X}}^{\mathrm{s}}/c_{\mathrm{X}}^{\mathrm{l}} = \exp\ \{[\tilde{\mu}_{\mathrm{X}}^{\mathrm{l}}(p, T_{\mathrm{m}}) - \tilde{\mu}_{\mathrm{X}}^{\mathrm{s}}(p, T_{\mathrm{m}})]/k_{\mathrm{B}}T_{\mathrm{m}}\}. \quad (40)$$

In general $\tilde{\mu}_{\mathrm{X}}^{l} < \tilde{\mu}_{\mathrm{X}}^{\mathrm{s}}$, because the greater mobility of the liquid can usually better accommodate particles of solute, and therefore their energy (chemical potential) is lower. This means that the concentration of the solute is usually smaller in the solid.

4.1.2. First principles calculations of chemical potentials. To calculate μ_{X} it is useful to consider the difference in chemical potential between the solute and the solvent $\mu_{\mathrm{XA}} = \mu_{\mathrm{X}} - \mu_{\mathrm{A}}$, which is equal to the change of Helmholtz free energy of the system as one atom of solvent is transmuted into an atom of solute at constant volume V and constant temperature p. Here the solvent is Fe and the solute one of the three impurities considered S, Si or O. This transmutation does not obviously correspond to a real physical process, but provides a perfectly rigorous way of calculating the difference of chemical potentials:

$$\mu_{\mathrm{XA}} = k_{\mathrm{B}}T\ \ln\ \frac{c_{\mathrm{X}}}{1 - c_{\mathrm{X}}} + 3k_{\mathrm{B}}T\ \ln\ (\Lambda_{\mathrm{X}}/\Lambda_{\mathrm{A}}) + m(c_{\mathrm{X}}), \quad (41)$$

where Λ_{X} and Λ_{A} are the thermal wavelengths of solute and solvent, and

$$m(c_{\mathrm{X}}) = -k_{\mathrm{B}}T\ \ln\ \frac{\int_V \mathrm{d}\mathbf{R}\ \exp\ [-\beta U(N_{\mathrm{A}} - 1, N_{\mathrm{X}} + 1; \mathbf{R})]}{\int_V \mathrm{d}\mathbf{R}\ \exp\ [-\beta U(N_{\mathrm{A}}, N_{\mathrm{X}}; \mathbf{R})]}, \quad (42)$$

with $U(N_A, N_X; \mathbf{R})$ the potential energy of the system with N_{A} atoms of solvent and N_{X} atoms of solute, and $U(N_A - 1, N_X + 1; \mathbf{R})$ the one for the system in which one of the atoms of solvent has been transmuted into solute. Since we will be interested in differences of chemical potentials between solid and liquids, the term $3k_{\mathrm{B}}T\ \ln\ (\Lambda_{\mathrm{X}}/\Lambda_{\mathrm{A}})$ cancels out and can therefore be ignored for this purpose.

The thermodynamic integration technique described in section 3.2 can now be used to compute $m(c_{\mathrm{X}})$ in the liquid state. This is done by defining an intermediate potential $U_\lambda = \lambda U(N_A - 1, N_X + 1; \mathbf{R}) + (1 - \lambda)U(N_A, N_X; \mathbf{R})$, so that $m(c_{\mathrm{X}})$ can be expressed as

$$m(c_{\mathrm{X}}) = \int_0^1 \mathrm{d}\lambda \langle U(N_{\mathrm{A}} - 1, N_{\mathrm{X}} + 1) - U(N_{\mathrm{A}}, N_{\mathrm{X}})\rangle_\lambda. \quad (43)$$

In practice, the calculation of $m(c_{\mathrm{X}})$ is done by performing two separate simulations, one with N_{A} atoms of solvent and N_{X} of solute and the other with $N_{\mathrm{A}} - 1$ atoms of solvent and $N_{\mathrm{X}} + 1$ atoms of solute. At the end of each time step forces are computed in both systems, and their linear combination $f_\lambda = \lambda f\ (N_{\mathrm{A}} - 1, N_{\mathrm{X}} + 1) + (1 - \lambda)f(N_{\mathrm{A}}, N_{\mathrm{X}})$ is used to evolve the system in time in order to compute the thermal average $\langle U(N_{\mathrm{A}} - 1, N_{\mathrm{X}} + 1) - U(N_{\mathrm{A}}, N_{\mathrm{X}})\rangle_\lambda$. This is repeated at a number of different values of λ and the integral is performed numerically.

To improve statistics, it is useful to transmute many atoms of solvent into solute. In this case one does not obtain directly μ_{XA} at a chosen concentration, but an integral of this over a range of concentrations. However, by repeating the calculations transmuting a different number of atoms at a time, it is possible to extract information about the value of μ_{XA} in a whole range of concentration, as described in [56].

In the solid state, thermodynamic integration is not the most appropriate way of calculating the chemical potential difference μ_{XA}. This is clear, because in the zero temperature limit, at infinite dilution $m(c_{\mathrm{X}} \to 0)$ is simply the change in internal energy when one atom in the perfect lattice of solvent is replaced by a solute atom, the impurity system being relaxed to equilibrium. At finite temperatures in the infinite dilution limit, $m(c_{\mathrm{X}} \to 0)$ can be obtained from the quasi-harmonic vibrational frequencies of the pure A system and the system containing a single X impurity. If anharmonic effects are significant, as they are in the case of O substituted in solid hexagonal closed packed Fe [57], thermodynamic integration can be used to estimate the anharmonic effects. These methods can also be generalized to include the variation of $m(c_{\mathrm{X}})$ with c_{X} to linear order in c_{X} [56].

The evaluation of $m(c_{\mathrm{X}})$ only gives access to the difference between the chemical potential of the solute and that of the solvent. However, we can obtain μ_{X} by our knowledge of μ_{A}, in our case the free energy of pure Fe, which we know from the discussion in section 3.

Equation (40) can now be used to put constraints on the composition of the Earth's core [56,58,59]. The constraints came from a comparison of the calculated density contrast at the inner core boundary, and that obtained from seismology, which is between $4.5 \pm 0.5\%$ [60] and $6.5 \pm 1.4\%$ [5]. This density contrast is significantly higher than that due to the crystallization of pure iron (which is 1.8% according to first principles calculations [51]), and therefore must be due to the partitioning of light elements between solid and liquid. As mentioned above, here we considered sulphur, silicon and oxygen as possible impurities. The results are summarized in figure 6. The top panel shows the density of the liquid core as a function of concentration of light impurities Si, S and O. For example, if O is the chosen light impurity, the figure shows that it is necessary to put 18% of O in liquid Fe to match the density of the core. The mid panel shows the relation between the concentration of impurities in solid and liquid. Here two main behaviours are apparent: for S and Si the two concentrations are almost identical, while O hardly goes

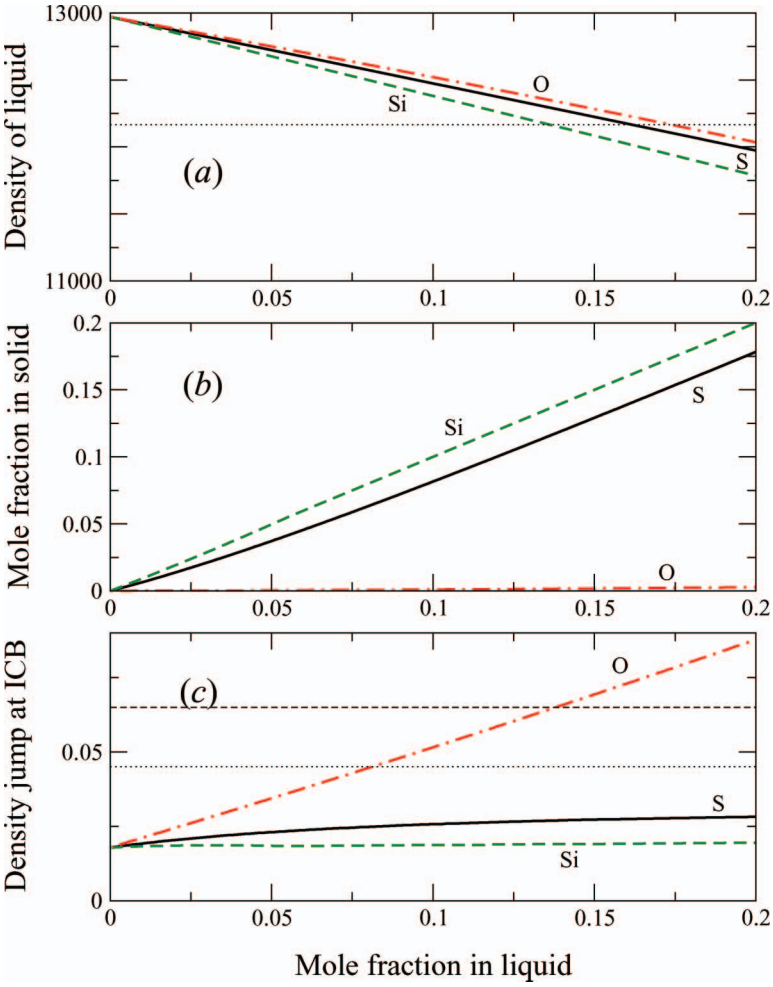

Figure 6. Liquid and solid impurity mole fractions c_X^l and c_X^l of impurities X = S, Si and O, and resulting densities of the inner and outer core of the Earth predicted by first-principles simulations. Solid, dashed and chain curves represent S, Si and O, respectively. (*a*) Liquid density ρ^l (kg m^{-3} units); horizontal dotted line shows density from seismic data [3,60]; (*b*) mole fractions in solid resulting from equality of chemical potentials in solid and liquid; (*c*) relative density discontinuity $\delta\rho/\rho^l$ at the ICB; horizontal dotted and dashed lines are values from free oscillation data [5,60]. Adapted from [58], with permission. Copyright 2002 Elsevier.

into the solid. The bottom panel used the results displayed in the mid panel to obtain the density jump at the ICB. Since the concentration of S and Si is almost the same in solid and liquid, the density contrast of a Fe/S or a Fe/Si system is not much different from that of pure Fe, and is still too low when compared with the seismological data. By contrast, for oxygen the partitioning between solid and liquid is very large, and this results in a much too large density contrast, which also does not agree with the seismological data.

The conclusion from these calculations is that *none of these binary mixtures can be viable for the core*. The density contrast can of course be explained by ternary or quaternary mixtures. Assuming no cross-correlated effects between the chemical potentials of different impurities, and based on the seismological density contrast of 4.5 ± 0.5% [60] we [56,58] proposed an inner core containing about 8.5% of sulphur and/or silicon and almost no oxygen, and an outer core containing about 10% of sulphur and/or Si, and an additional 8% of oxygen. The more recent seismological datum of 6.5 ± 1.4% [5] would change the estimate of the core composition to an inner core containing about 7% of sulphur and/or silicon and still almost no oxygen, and an outer core containing about 8% of sulphur and/or Si, and an additional 13% of oxygen. One consequence of the large partitioning of oxygen between solid and liquid is that as the solid core grows it expels oxygen in the liquid, which by converting its gravitational energy helps driving the convective motions that are responsible for the generation of the Earth's magnetic field [61].

4.1.3. Shift of freezing point. The partitioning of the solute between the solid and the liquid is generally responsible for a change in the melting temperature of the mixture with respect to that of the pure solvent. This is because the solute usually finds better accommodation in the liquid, and this flow from the solid to the liquid is responsible for a decrease of the Gibbs free energy of the liquid with respect to that of the solid. This lowering of Gibbs free energy in the liquid produces a depression of the freezing point. This is the reason why, for example, sea water freezes only when the temperatures are well below zero, it is because of the salt dissolved into it. Similarly, this effect is commonly exploited to reduce the formation of ice on public roads by the spreading of salt. The dissolution of salt lowers the freezing point of water. If the concentration of solute is small, the depression of the freezing point is given by

$$\delta T = \frac{kT_{\mathrm{m}}}{\Delta s}(c_{\mathrm{X}}^{\mathrm{s}} - c_{\mathrm{X}}^{\mathrm{l}}), \tag{44}$$

where Δs is the entropy change on melting of the pure solvent and T_{m} is the melting temperature of the pure solvent.

Using equation (44), and the composition estimated from the density contrast of 4.5% we can now estimate a depression of about 600 – 700 K of the melting temperature of the core mixture with respect to the melting temperature of pure Fe, which would produce an inner-core boundary temperature of about 5700 K. This estimate would go down by a further 300 K if the latest estimate of 6.5% for the density contrast at ICB was used [5], which would therefore result in a temperature at the ICB of about 5400 K. Combining this with equation (1), which describes the variation of temperature with depth assuming that the temperature distribution is adiabatic, we can also obtain an estimate for the temperature at the top of the core, which is approximately equal to 4000 K.

5. Summary

We have discussed in this paper the development of a number of first principles calculations techniques used to infer the properties of the Earth's core. These techniques are based on the fundamental laws of nature as described by quantum mechanics. In particular, we have shown that it is possible to calculate chemical potentials from first principles, and that with the knowledge of these chemical potentials for a number of pretenders it is possible to estimate the temperature and the composition of the Earth's core. We have described that these results can be obtained by combining experimental knowledge about the Earth's core, mainly from seismic observations, with first principles calculations. The first seismic observation which comes into play is the discovery of a solid and a liquid core, and therefore a boundary between the two (the ICB). Thermodynamic equilibrium between solid and liquid at the ICB can be used to estimate the temperature of the ICB. The additional seismic observations of the density jump at the ICB can be used to put constraints on the composition of the Earth's core. We have shown that these constraints result in an ICB temperature of 5400 – 5700 K, and require the presence of a significant amount of oxygen in the liquid core. This oxygen is expelled by the mixture with Fe as the ICB grows, and its gravitational energy becomes available to maintain the convective motions in the liquid core which are responsible for the generation of the Earth's magnetic field. The estimate of the temperature of the Earth's core provides a fixed point that can be used to infer the thermal structure of the core, which in turn can be used to understand better convection and heat transfer. The results of this work are graphically summarized in figure 7.

The reliability of these results is supported by the large amount of experimental data that first principles calculations reproduce very accurately. Here we have only mentioned a very limited number of these. The robustness of first principles calculations gives confidence that they have useful predictive power, and they can even be used in regions where experiments cannot be performed. In particular, in the present discussion density functional theory has been the first principles tool of choice, as it has shown to be a very reliable instrument to predict the thermodynamic properties of iron.

We conclude by reminding that we focused our discussion on the thermodynamic properties of a rather limited set of light impurities, i.e. S, Si and O, and based our estimate for a core composition on these elements only, because these three are thought to be the most likely

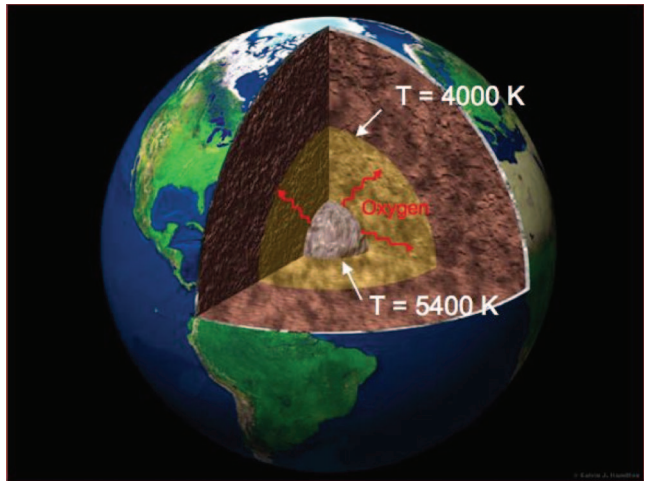

Figure 7. Schematic summary of the results presented in this article for the temperature and composition of the Earth's core.

candidates to be in the core. In principle other elements like C and H have been proposed as possible light elements in the core, so a possible natural development of this research could be to apply the techniques discussed here to look at these other light elements too.

Acknowledgements

The work was conducted as part of a EURYI scheme award as provided by EPSRC (see www.esf.org/euryi).

References

[1] Wikipedia. Available online at: http://en.wikipedia.org/wiki/Kola_Superdeep_Borehole.
[2] D.J. Stevenson, Nature **423** 239 (2003).
[3] A.M. Dziewonski and D.L. Anderson, Phys. Earth Planet. Inter. **25** 297 (1981).
[4] C.J. Allègre, J.-P. Poirier, E. Humler, *et al.*, Planet. Sci. Lett. **134** 515 (1995).
[5] T.G. Masters and D. Gubbins, Phys. Earth Planet. Inter. **140** 159 (2003).
[6] O.L. Anderson, L. Dubrovinsky, S.K. Saxena, *et al.*, Geophys. Res. Lett. **28** 499 (2001).
[7] O.L. Anderson and A. Duba, J. Geophys. Res. Sol. Earth, **102** 22659 (1997).
[8] R. Boehler, Nature **363** 534 (1993).
[9] S.K. Saxena, G. Shen, and P. Lazor, Science, **264** 405 (1994).
[10] G. Shen, H. Mao, R.J. Hemley, *et al.*, Geophys. Res. Lett. **25** 373 (1998).
[11] Q. Williams, R. Jeanloz, J.D. Bass, *et al.*, Science **286** 181 (1987).
[12] S.K. Saxena and L.S. Dubrovinski, Am. Mineral. **85** 372 (2000).
[13] Y. Ma, M. Somayazulu, G. Shen, *et al.*, Phys. Earth Planet. Int., **143–144** 455 (2004).
[14] L.R. Benedetti, N. Guignot, D.L. Farber, J. App. Phys. **101** 013109 (2007)
[15] C.S. Yoo, N.C. Holmes, M. Ross, *et al.*, Phys. Rev. Lett. **70** 3931 (1993).
[16] J.M. Brown and R.G. McQueen, J. Geophys. Res. **91** 7485 (1986).
[17] J.H. Nguyen and N.C. Holmes, Nature **427** 339 (2004).
[18] P. Hohenberg and W. Kohn, Phys. Rev. **136** B864 (1964).
[19] W. Kohn and L. Sham, Phys. Rev. **140** A1133 (1965).
[20] N.D. Mermin, Phys. Rev. **137** A1441 (1965).
[21] D.R. Bowler, T. Miyazaki and M.J. Gillan, J. Phys.: Condens. Matter **14** 2781 (2002).
[22] J.M. Soler, E. Artacho, J.D. Gale, *et al.*, J. Phys.: Condens. Matter **14** 2745 (2002).
[23] P.Y. Savrasov and G. Kotliar, Phys. Rev. Lett. **90** 056401 (2003).
[24] W.M.C. Foulkes, L. Mitaš, R.J. Needs, *et al.*, Rev. Mod. Phys. **73** 33 (2001).
[25] R.G. Parr and W. Yang, *Density-Functional Theory ofAtoms and Molecules* (Oxford Science Publications, Oxford, 1989).
[26] R.M. Dreizler and E.K.U. Gross, *Density Functional Theory* (Springer-Verlag, Berlin, 1990).
[27] R.M. Martin, *Electronic Structure* (Cambridge University Press, Cambridge, 2004).
[28] M.J. Gillan, Contemp. Phys. **38** 115 (1997).
[29] D. Ceperley and B. Alder, Phys. Rev. Lett. **45** 566 (1980).
[30] J.P. Perdew and A. Zunger, Phys. Rev. B **23** 5040 (1981).
[31] Y. Wang and J. Perdew, Phys. Rev. B **44** 13298 (1991).
[32] J. Tao, J.P. Perdew, V.N. Staroverov, *et al.*, Phys. Rev. Lett. **91** 146401 (2003).
[33] V.N. Staroverov, G.E. Scuseria, J. Tao, *et al.*, Phys. Rev. B **69** 075102 (2004).
[34] A.D. Becke, J. Chem. Phys. **98** 5648 (1993).
[35] D.R. Hamann, M. Schlüter and C. Chiang, Phys. Rev. Lett. **43** 1494 (1979).
[36] G.P. Kerker, J. Phys. C **13** L189 (1980).
[37] G.B. Bachelet, D.R. Hamann and M. Schlüter, Phys. Rev. B **26** 4199 (1982).
[38] D. Vanderbilt, Phys. Rev. B **41** 7892 (1990).
[39] P.E. Blöchl, Phys. Rev. B **50** 17953 (1994).
[40] G. Kresse and D. Joubert, Phys. Rev. B **59** 1758 (1999).
[41] G. Kresse and J. Furthmuller, Comput. Mater. Sci. **6** (1996) 15; Phys. Rev. B **54**(1996) 11169.
[42] D. Alfè, G.D. Price and M.J. Gillan, Phys. Rev. B **64** 045123 (2001).
[43] G. Kresse, J. Furthmüller and J. Hafner, Europhys. Lett. **32** 729 (1995).
[44] D. Alfè. Program Available online at: http://chianti.geol.ucl.ac.uk/~dario (1998).
[45] P. Giannozzi, S. de Gironcoli, P. Pavone, *et al.*, Phys. Rev B **43** 7231 (1991).
[46] S. Baroni, P. Gianozzi and A. Testa, Phys. Rev. Lett. **58** 1861 (1987).
[47] S. Baroni, S. de Gironcoli, A. Dal Corso, *et al.*, Rev. Mod. Phys. **73** 515 (2001).
[48] X. Gonze and J.-P. Vigneron, Phys. Rev. B **39** 13120 (1989).
[49] D. Alfè, G. Kresse and M.J. Gillan, Phys. Rev. B **61** 132 (2000).
[50] D. Frenkel and B. Smit, *Understanding Molecular Simulation* (Academic Press, San Diego, 1996).
[51] D. Alfè, M.J. Gillan and G.D. Price, Phys. Rev. B **65** 165118 (2002).
[52] D. Alfè, M.J. Gillan and G.D. Price, Nature **401** 462 (1999).
[53] D. Alfè, G.D. Price and M.J. Gillan, J. Chem. Phys. **116** 6170, (2002).
[54] G.H. Wannier, *Statistical Physics* (Dover Publications, Inc., New York, 1966).
[55] F. Mandl, *Statistical Physics*, 2nd edn. (John Wiley & Sons, New York, 1997).
[56] D. Alfè, G.D. Price and M.J. Gillan, J. Chem. Phys. **116** 7127 (2002).
[57] D. Alfè, G.D. Price and M.J. Gillan, Geophys. Res. Lett. **27** 2417 (2000).
[58] D. Alfè, M.J. Gillan and G.D. Price, Earth and Planet. Sci. Lett. **195** 91 (2002).
[59] D. Alfè, G.D. Price and M.J. Gillan, Nature **405** 172 (2000).
[60] T.G. Masters and P.M. Shearer, J. Geophys. Res. **95** 21691 (1990).
[61] D. Gubbins, D. Alfè, G. Masters, *et al.*, Geophys. J. Intern. **157** 1407 (2004).

Dario Alfè is Professor of Physics at UCL. He obtained his PhD in Condensed Matter Physics from SISSA in 1997, Trieste, and became interested in Earth's science problems with his first post-doc at Keele University. He moved to UCL in 1998 where

he has been a Royal Society University Research Fellow between 2000 and 2006. Most of his work at UCL has been devoted to development and application of novel first-principles techniques for study of solids and liquids over a wide range of conditions of pressure and temperature. He was awarded the Philip Leverhulme Prize and the Doornbos Memorial Prize in 2002, the EPSRC High Performance Computing Prize in 2005, and the European Young Investigator Award (EURYI) in 2005.

Mike Gillan is Professor of Physics at UCL. He received a DPhil. in theoretical physics from the University of Oxford in 1968, spent two years as a post-doc at the University of Minnesota, and then worked until 1988 in the Theoretical Physics Division at AERE Harwell. He then went to Keele University as Professor of Theoretical Physics and before moving to UCL in 1998 he became interested in the physics of the Earth's core. He was awarded the Institute of Physics Dirac Medal in 2006 which recognizes excellence in theoretical or computational physics.

G. David Price is Executive Dean of the Mathematical and Physical Sciences Faculty of UCL and Professor of Mineral Physics. In 1983, he was one of the first to establish the now major field of computational mineral physics. He was awarded the Schlumberger Medal of the Mineralogical Society of Great Britain in 1999, the Murchison Medal of the Geological Society of London in 2002; and in 2006 he was awarded the Louis Néel Medal of the European Geosciences Union for 'establishing the importance of computational mineral physics in Earth sciences and for outstanding contributions to the physics of the Earth's core'. He is a Member of the Academia Europaea and a Fellow of the American Geophysical Union. He is an editor of *Earth and Planetary Science Letters*, and was President of the Mineralogical Society of Great Britain and Ireland (2004–2006).